X-ray diffraction characterization of ternary artificial superlattices

I. Goldfarb, E. Zolotoyabko, and D. Shechtman
Department of Materials Engineering, Technion-Israel Institute of Technology, Haifa 32000, Israel

(Received 23 October 1992; accepted for publication 10 May 1993)

Thin films of alternating Au, Ag, and Cu wedge-shaped metal layers were made by magnetron sputtering in order to develop a method for investigation of a multicomponent systems. X-ray-diffraction patterns of all as-deposited samples revealed satellites in the vicinity of (111) reflections, evidence of composition-modulated artificial superlattice formation. The experimental spectra are well explained by the kinematical diffraction theory for imperfect superlattices. Computer simulations have demonstrated extremely high sensitivity to the fluctuations $\Delta H/H$ of the superlattice period H. As a result, a rapid and simple method of $\Delta H/H$ determination is proposed.

I. INTRODUCTION

Artificial superlattices attract attention due to the possibility of "tailoring" unusual properties on interfaces with reduced dimensionality. Applications were found in mirror production for soft-x-ray and ultraviolet radiations.[1–4] The preparation of conventional flat layered superlattices involves an alternating vacuum deposition (although lately an electrochemical method has also been applied[5]) of components providing control of layer thickness on the atomic level and absence of interdiffusion at the interfaces. Molecular-beam epitaxy (MBE) is indeed a favorable method, but in an effort to reduce the production costs other vacuum deposition methods, such as electron gun (EG) evaporation, chemical-vapor deposition (CVD), and sputtering are also in common use.[4]

New advantages arise when wedge-layered superlattices are prepared. For example a set of samples with continuously varied concentration of the components can be produced simultaneously. This set may be used in order to investigate various properties as well as the phase diagram of multicomponent systems. For this purpose the samples should be annealed at elevated temperatures to provide component mixing by interdiffusion. Deviations from phase compositions and from related properties, when compared to systems produced by conventional methods, will be subjected to investigation. The authors have applied the proposed method in the well-known[6–8] Au-Ag-Cu ternary system. As a first stage, we present here the results of x-ray-diffraction (XRD) characterization of as-deposited wedge-shaped Au-Ag-Cu superlattice layers, produced by magnetron sputter deposition.

The term "superlattice" is used in the sense that atomic positions inside the multilayered structure are correlated (at least in one direction) across several layers, and such correlations are revealed as satellites in the high-angle region of the diffraction pattern.

II. SAMPLE PREPARATION AND EXPERIMENTAL PROCEDURES

Preparation of wedge-layered superlattices was performed in a magnetron sputtering system equipped with a water-cooled rotating substrate table, dc and rf generators of 1 kW, and a substrate shutter for gradual deposition. High-purity Ar was used to form a dc plasma for sputtering off 3 in. 99.99% Au, Ag, and Cu targets. Prior to deposition the sputtering chamber was evacuated to 1.3×10^{-5} Pa, 0.4 Pa of Ar was introduced, and the target was presputtered for 30 min, with closed target shutters. Following several Ar flushes, the sputtering began with a dynamic pressure of 0.4 Pa.

Electron microscope molybdenum grids (100 mesh), coated with Formvar, were used as substrates in this study. 55 grids were arranged in a close-packed equilateral triangle and covered by the substrate shutter, as shown in Fig. 1. The substrate table was then located under an open Ag target, with one of the triangle sides parallel to the edge of the shutter (see Fig. 1). The sputtering began with 30 W power. Simultaneously, the shutter moved along the triangle altitude, and the sputtering was terminated when the shutter reached the triangle basis. The triangular substrate was then rotated 120° until a second triangle side was parallel to the shutter edge, and a shutter was closed again. Following that, the substrate table was located under the Au target and the process was repeated with different power. The same procedure followed under the Cu target. The sputtering power for each target was determined by experimental calibration to give the same thickness (120 Å) at the thick edge of sputtered film, namely 30 W for Au and Ag, and 61 W for Cu. The thickness of each component is linearly reduced from the apex along the triangle altitude, and is practically zero at the triangle basis. As a result, a 120-Å-thick Ag-Au-Cu triple layer (trilayer) was formed in the manner shown in Fig. 2. A complete set consists of 55 grids covered with 30 trilayers providing 55 differently composed samples.

The local compositions were determined by scanning electron microscopy (SEM) equipped with a standard energy-dispersive spectroscopy (EDS) attachment. Each sample was analyzed at several points for an average concentration, using 5 kV accelerating voltage to prevent the excitation of the substrate. A standard ZAF (Z number, absorption, fluorescence) correction using M and L characteristic lines was used for the EDS analysis. The composition of relevant samples is shown in Table I.

The XRD spectra of the samples were measured in

 0021-8979/93/74(4)/2501/6/$6.00

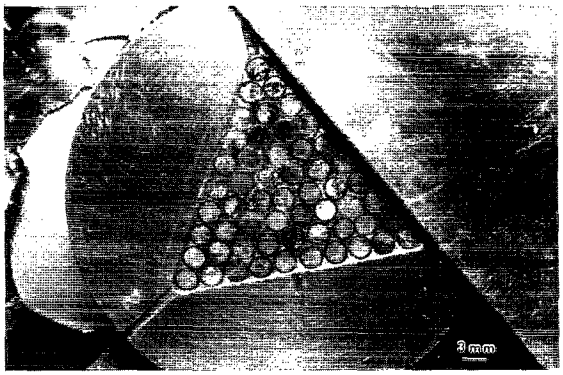

FIG. 1. Experimental configuration of the substrates in the sputtering chamber: the substrates are on the table and the shutter is open.

TABLE I. Atomic concentrations of some relevant samples measured by energy-dispersive spectroscopy.

Sample	at. % Au	at. % Ag	at. % Cu
1	8	77	15
3	7	65	28
5	14	57	29
6	7	56	37
8	20	57	23
9	15	50	35
12	30	45	25
15	11	49	40
18	27	41	32
23	42	31	27
27	22	24	54
41	35	21	44
42	29	17	54
55	15	7	78

Bragg–Brentano parafocusing geometry, using a conventional x-ray diffractometer, equipped with bent graphite monochromator and Cu radiation tube. Each scan was performed in a step mode with step size $\Delta 2\theta = 0.035°$ and 10 s of exposure per step.

III. XRD DATA

In the first stage pure Au, Ag, and Cu films were sputtered as standards for the various analytical methods. Their XRD patterns exhibited a clearly pronounced (111) preferred orientation [see Figs. 3(a)–3(c)], as is usually the case with physical-vapor-deposition (PVD) -deposited fcc metals.[9,10] The same effect was observed in all trilayered samples, as demonstrated in Fig. 4, where a typical XRD pattern is shown. This strong preferred orientation leads to single crystal-like behavior of diffraction response from (111) atomic planes. For instance, one should expect the modulation of (111) reflection intensity due to the superlattice period provided a superlattice of a good enough quality is formed. This means that possible imperfections in the interfaces between the layers of different metals do not completely destroy right-phase relations between the scattered waves. Actually, such a modulation is observed for all samples in the vicinity of (111) peaks and typical spectra are shown in Fig. 5.

The main features of the collected data are described here. The shape of each spectrum is determined by the relationship between the position of bulk reflections, defined by Bragg law,

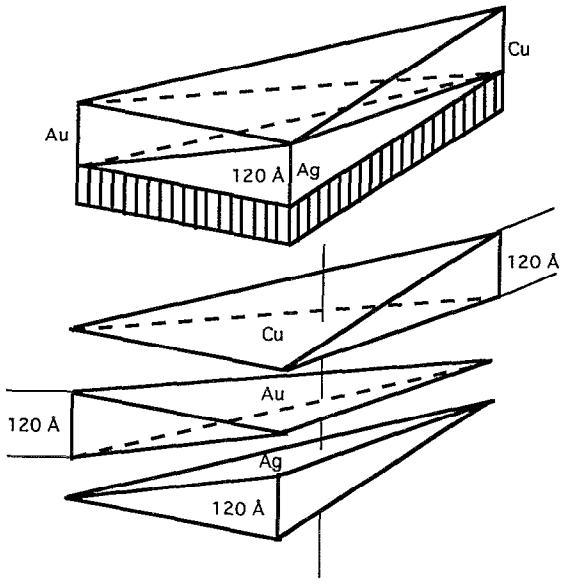

FIG. 2. Schematic representation of the prismatic Au-Ag-Cu trilayer.

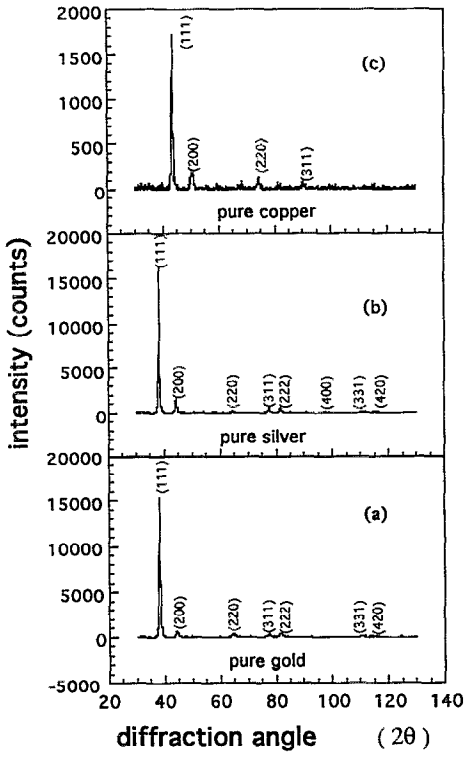

FIG. 3. X-ray diffraction patterns of pure Au, Ag, and Cu, exhibiting a strong {111} preferred orientation.

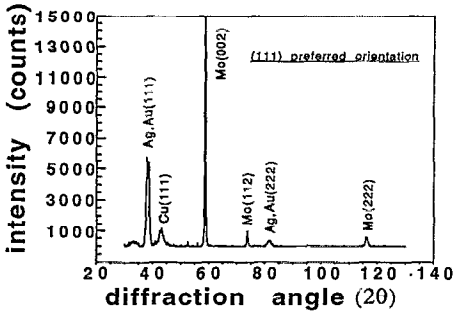

FIG. 4. An example of a typical (111)-oriented trilayered sample (sample 41). The Mo reflections are from the substrate.

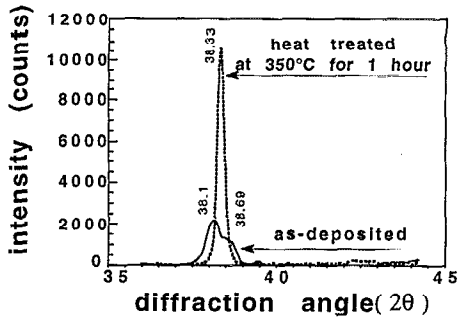

FIG. 6. The result of heat treatment is the complete destruction of the modulated structure as seen by the absence of satellites.

$$Qd_i/2=\pi \tag{1}$$

(where $Q=4\pi \sin\theta/\lambda$ is the diffraction vector, λ is the x-ray wavelength, and d_i is the interplanar spacing for the ith metallic lattice) and by the satellite angular positions defined by the triple "sandwich" thickness (superperiod) H as[11]

$$QH/2=k\pi, \tag{2}$$

where $k=0, 1, 2,\ldots$. When

$$H/d_i=k, \tag{3}$$

it specifies the coincidence of a bulk reflection with the kth satellite. This fact leads to the corresponding amplification of the bulk reflection. In the opposite case when

$$H/d_i=k+\tfrac{1}{2}, \tag{4}$$

a diffraction spectrum is obtained with satellites located symmetrically around a reduced bulk reflection, as shown in Fig. 5(c). Intermediate situations [between Eqs. (3) and (4)] provide an asymmetrical diffraction pattern with satellites shifted to the right- or to the left-hand side of the bulk reflection, as demonstrated in Figs. 5(a) and 5(b). It follows that a superimposed diffraction pattern is very sensitive to the variations of H, which can be determined from the observed angular distance ($2\Delta\theta$) between the satellites by the expression

$$H=\lambda/(2\Delta\theta \cos\theta_B) \tag{5}$$

(where θ_B is the Bragg angle for the reflection used), which follows directly from Eq. (2). Thus, the measurement of the positions of satellites provides an important tool for the precise determination of H. In our case the value of $H=125$ Å was found, which is close to the expected value ($H=120$ Å) from the sputtering conditions.

Since the lattice constants of Ag and Au are very close, but differ considerably from the Cu lattice constant, it is expected that variations in H are connected mainly to the relative concentration of Cu. Thus, the characteristic shape of diffraction profile will not change substantially at fixed Cu concentration (independent of the relative Au/Ag concentration), as is demonstrated clearly in Figs. 5(a) and 5(b).

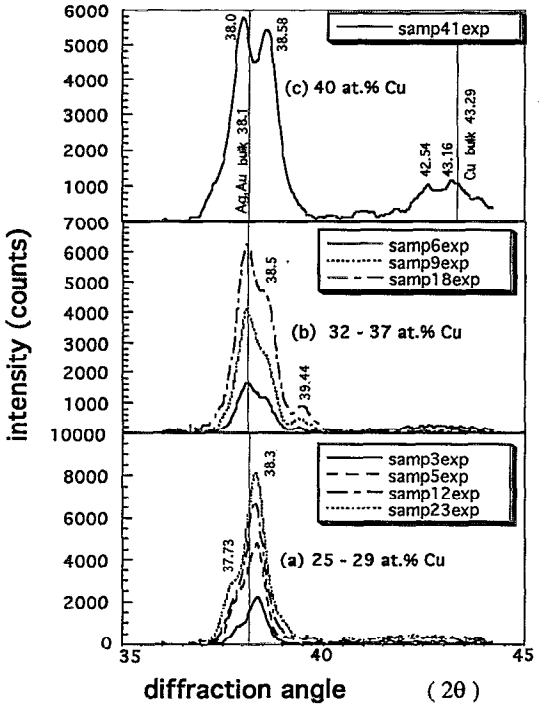

FIG. 5. Typical modulated diffraction pattern in the vicinity of the Au, Ag (111) bulk reflection: (a) 25–29 at. % Cu; (b) 32–37 at. % Cu; (c) 40 at. % Cu. "exp" stands for "experimental."

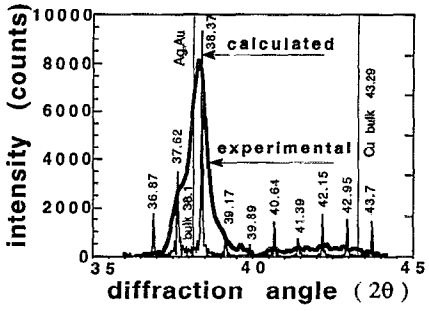

FIG. 7. The calculated spectrum based on the perfect superlattice theory superimposed on the experimental x-ray-diffraction pattern (sample 23).

An additional confirmation of the superlattice formation in the as-deposited samples comes from XRD of the heat-treated samples where a complete destruction of the superlattice due to the interdiffusion takes place. A typical result of the heat treatment is shown in Fig. 6. In sample 1, heat treated in vacuum for 1 h at 350 °C, only a strong symmetric (111) reflection from the Ag-rich solid solution is present with no traces of satellites. More detailed superlattice characterization can be achieved by means of a computer fitting procedure which is described next, in Sec. IV.

IV. COMPUTER SIMULATIONS AND DISCUSSION

For an ideal superlattice the diffraction intensity can be calculated by means of direct summation of waves (with corresponding phases) scattered by the array of atomic planes. In the case of binary superlattices such calculations have been performed by several authors.[4,12] Here we extend the theoretical description to the ternary superlattices. For thin films the kinematic approximation is sufficient without, taking into account multiple scattering effects. This is the case in our study, since the extinction length, even for the Au (111) reflection, is 1.8 μm, i.e., substantially larger than the total sample thickness, which is $T=NH\approx 0.36$ μm, where N designates the number of triple layers. Wave summation over a Au-Ag-Cu layered superlattice, with real interlayer order, leads to the following expression for the square of the structure factor, which is proportional to the diffracted intensity:

$$\begin{aligned}|F(Q)|^2=\{&f_{\mathrm{Cu}}^2L_{\mathrm{Cu}}+f_{\mathrm{Au}}^2L_{\mathrm{Au}}+f_{\mathrm{Ag}}^2L_{\mathrm{Ag}}+2f_{\mathrm{Cu}}f_{\mathrm{Au}}(L_{\mathrm{Cu}}L_{\mathrm{Au}})^{1/2}\cos[Q(d_{\mathrm{Cu}}n_{\mathrm{Cu}}+d_{\mathrm{Au}}n_{\mathrm{Au}})/2]\\&+2f_{\mathrm{Cu}}f_{\mathrm{Au}}(L_{\mathrm{Cu}}L_{\mathrm{Au}})^{1/2}\cos[Q(d_{\mathrm{Cu}}n_{\mathrm{Cu}}+2d_{\mathrm{Au}}n_{\mathrm{Au}}+d_{\mathrm{Ag}}n_{\mathrm{Ag}})/2]\\&+2f_{\mathrm{Ag}}f_{\mathrm{Au}}(L_{\mathrm{Ag}}L_{\mathrm{Au}})^{1/2}\cos[Q(d_{\mathrm{Ag}}n_{\mathrm{Ag}}+d_{\mathrm{Au}}n_{\mathrm{Au}})/2]\}L,\end{aligned}\tag{6}$$

where f_i, n_i are the atomic formfactor and number of atomic planes of the ith component in a trilayer, respectively,

$$L_i=[\sin(Qd_in_i/2)/\sin(Qd_i/2)]^2\tag{7}$$

is the Laue interference function for the ith component, and

$$L=[\sin(QHN/2)/\sin(QH/2)]^2\tag{8}$$

is the Laue interference function for the superlattice, where $H=\Sigma_i n_i d_i$. In the derivation process of Eq. (6), the interface thickness is assumed to be $(d_i+d_j)/2$. In the limit, when f_i or n_i approaches zero, Eq. (6) transforms to the well-known[4] expression for a two-component system. Note also that zero in the denominators of Eqs. (7) and (8) leads to the Bragg conditions (1) and (2). Computer simulation based on Eq. (6) shows that the positions of spectral features can be fitted very well to an H variation. An example of such a fitting is presented in Fig. 7. The accuracy δH of H determination is sufficiently high, and can be evaluated considering the transformation of the diffraction pattern from mode (3) to mode (4). The transition mentioned occurs when H is varied as

$$\delta H=d/2.\tag{9}$$

In our case ($d^{(111)}{}_{\mathrm{Au}}\approx 2.3$ Å) expression (9) gives the estimation of $\delta H=1$ Å.

The next step of the fitting procedure consists of the introduction of a broadening mechanism for narrow diffraction peaks resulting from Eq. (6). In other words, some imperfection must be introduced into the theory for an ideal superlattice. There are several ways of doing this,[4] however, it is known that strong reflection broadening results from layer thickness fluctuations, which destroy the phase relations between scattered waves. The case of two-component systems was analyzed in detail in recent publications.[13,14] Analysis of ternary superlattices is more complicated due to the increased number of variable parameters. Our case is somewhat simplified because of a resemblance of Au and Ag lattice parameters [the mismatch $\eta_1=(d_{\mathrm{Ag}}-d_{\mathrm{Au}})/d_{\mathrm{Ag}}\approx 0.2\%$]. Thus, the adjacent Au and Ag layers can be considered as completely matched, with no destruction of packing sequence along the [111] direction. On the countrary, large lattice mismatch [$\eta_2=(d_{\mathrm{Au}}-d_{\mathrm{Cu}})/d_{\mathrm{Au}}\approx 11\%$] between (Au, Ag) and Cu layers promotes defect formation on the corresponding interface and consequently leads to the fluctuations of the layer thickness and thus of the superlattice period $\Delta H/H$. As was previously mentioned, H variation strongly affects the diffraction pattern. In order to take into account $\Delta H/H$ fluctuations we used the approach[15] that modifies the expression for the Laue function (8) into the following form:

$$L^m(Q)=\frac{1+\exp(-N\sigma^2Q^2/2)-2\exp(-N\sigma^2Q^2/4)\cos(NHQ)}{1+\exp(-\sigma^2Q^2/2)-2\exp(-\sigma^2Q^2/4)\cos(HQ)},\tag{10}$$

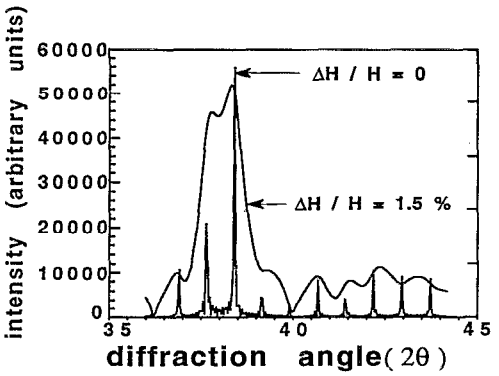

FIG. 8. Two superimposed calculated spectra for sample 23: with no thickness fluctuations ($\Delta H/H=0$), and with $\Delta H/H=1.5\%$.

where $\Delta H/H=1.67\sigma/H$. Replacement of Eq. (8) by Eq. (10) in Eq. (6) drastically changes the diffraction pattern as shown in Fig. 8. Varying the $\Delta H/H$ parameter, one can fit the calculated structure factor to an experimental data. The best fit of all samples was found to be $\Delta H/H=1.5\%$. Several examples of these results are demonstrated in Fig. 9. Note that a variation of 0.5% (around the best fit value of 1.5%) in $\Delta H/H$ reduces the fitting significantly [see Fig. 10 versus Fig. 9(a)].

Relative variation of $\Delta H/H=1.5\%$ corresponds to the thickness variation of $\Delta H=1.9$ Å, which approximately equals to one Cu monolayer in the [111] direction. Thus,

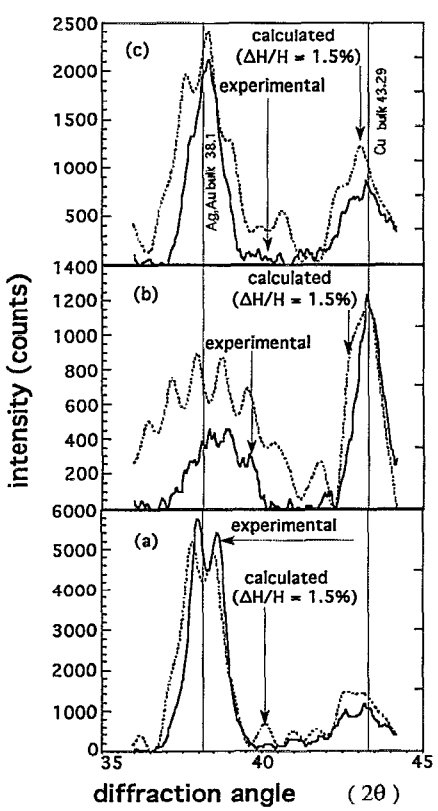

FIG. 9. Superimposed calculated and experimental spectra for $\Delta H/H=1.5\%$: (a) sample 41; (b) sample 55; (c) sample 27.

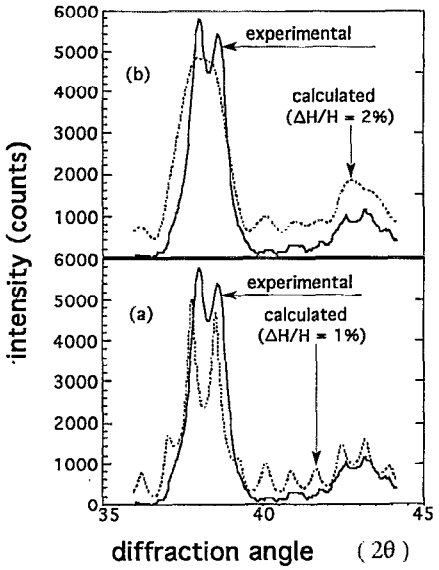

FIG. 10. The fitting of the calculated spectra to the experimental from sample 41: (a) $\Delta H/H=1\%$; (b) $\Delta H/H=2\%$ [compare to Fig. 9(a)].

the fluctuations of roughly a single monolayer, most probably on the (Au, Ag)-Cu interfaces, significantly broaden the diffraction spectrum in the high-angle region. However, there is still a partial conservation of modulation features due to the superlattice order. This conclusion coincides with the results of calculations for binary systems.[13,14]

Note also that the presence of a superlattice order in a case of $\eta\approx 11\%$ mismatch in adjacent (Au, Ag)-Cu layers is rather surprising. In fact, such a mismatch is close to the "boundary of stability" ($\eta_b=14\%$) of superlattice formation.[13] This value was derived from the observation of the diffraction satellites in, for example, Mo-Ni ($\eta=9\%$)[16] and Nb-Cu ($\eta=10.5\%$)[17] systems, as well as from the absence of satellites in Ti-Ni ($\eta=14\%$) and Zr-Ni ($\eta=21\%$) structures.[18] Our x-ray-diffraction data provide convincing proof that in the ternary Au-Ag-Cu system with $\eta=11\%$, some correlations in atomic positions across several (111) layers still remain, as was revealed by the observed modulation of the (111) diffraction profile. One-dimensional order in the packing sequence (high-textured samples) satisfies the conditions for this modulation, as was also established for binary systems (see, for example, Ref. 16).

V. CONCLUSIONS

Artificial ternary Au-Ag-Cu superlattices were made of wedge-shaped layers using magnetron dc sputtering. This method provides samples with continuously varied concentration of the components. The samples exhibit strong preferred orientation of (111) atomic planes being parallel to the film surface, with almost perfectly sequenced atomic rows along the [111] direction. This is the reason for the observed modulation of XRD spectra in the vicinity of (111) bulk reflections, due to the superlattice formation.

By measuring the angular positions of spectral features it is possible to determine the average superlattice period H with an accuracy of about 1 Å.

Computer simulations based on the developed kinematical diffraction theory for a real ternary system revealed a high sensitivity of the fitting procedure to the superperiod fluctuations $\Delta H/H$. The best fit for all samples in our study corresponds to the value of $\Delta H/H = 1.5\%$, which approximately equals one monolayer in a growth direction. The parameters H and $\Delta H/H$ of such a superlattice can be determined with a good precision through XRD. The value of $\Delta H/H$ is rather difficult to measure by other methods.

ACKNOWLEDGMENTS

The authors wish to express their gratitude to Dr. A. Berner for his advice and help in the field of EDS, and to Eli Levy for his dedicated help in the process of samples preparation. The support of the Louis Edelstein Center is gratefully acknowledged.

[1] B. J. Thaler and J. B. Ketterson, Phys. Rev. Lett. **41**, 336 (1978).
[2] E. M. Gyorgy, D. B. McWhan, J. E. Dillon, Jr., L. R. Walker, and J. V. Waszsak, Phys. Rev. B **25**, 6739 (1982).
[3] J. E. Henein and J. E. Hilliard, J. Appl. Phys. **54**, 728 (1983).
[4] T. Shinjo and T. Takada, Eds., *Metallic Superlattices* (Elsevier, Amsterdam, 1987).
[5] D. S. Lashmore and M. D. Dariel, J. Electrochem. Soc. Solid State Sci. Technol. **135**, 1218 (1988).
[6] A. Prince, Int. Mater. Rev. **33**, 314 (1988).
[7] R. Kikuchi, J. M. Sunches, D. de Fontaine, and H. Yamauchi, Acta Metall. **28**, 651 (1980).
[8] M. Nakagawa and K. Yasuda, J. Less-Common Met. **138**, 95 (1988).
[9] L. Eckertova, *Physics of Thin Films*, translated by P. Bratinka (Plenum, New York, 1977), p. 109.
[10] W. M. Paulson and J. E. Hilliard, J. Appl. Phys. **48**, 2117 (1977).
[11] W. J. Bartels, J. Hornstra, and D. J. Lobeek, Acta Crystallogr. A **42**, 539 (1986).
[12] E. Fullerton, I. Schuller, and Y. Bruynseraede, MRS Bull. **12**, 33 (1992).
[13] B. M. Clemens and J. G. Gay, Phys. Rev. B **35**, 9337 (1987).
[14] F. J. Lamelas, H. D. He, and R. Clarke, Phys. Rev. B **43**, 12 296 (1991).
[15] Y. Fujii, T. Ohnishi, T. Ishihara, Y. Yamada, K. Kawaguchi, N. Nakayama, and T. Shinjo, J. Phys. Soc. Jpn. **53**, 521 (1986).
[16] M. R. Khan, C. S. Chun, G. P. Felcher, M. Grimsditch, A. Kueny, C. M. Falco, and I. K. Schuller, Phys. Rev. B **27**, 7286 (1983).
[17] I. K. Schuller, Phys. Rev. Lett. **44**, 1597 (1980).
[18] B. M. Clemens, Phys. Rev. B **33**, 7615 (1986).